

## SCALAR NETWORK ANALYZER-TYPE APPROACH FOR A TEMPERATURE MEASUREMENT SYSTEM BASED ON MICROWAVE SAW RESONATORS

Ioana GIANGU<sup>1</sup>, Valentin BUICULESCU<sup>2</sup>, Mihai NIŞULESCU<sup>3</sup>, George LOJEWSKI<sup>4</sup>

*This paper presents the first scalar network analyzer used for temperature monitoring based on a surface acoustic wave resonator as temperature sensor. The proposed system consists of an interrogation path which generates a RF signal covering a broad bandwidth and a signal sensing path for converting the SAW resonator's response into the useful temperature information. Typical frequency coverage of the experimental system is 5.25 - 6.05 GHz. Excepting the voltage controlled oscillator evaluation board, all other components - high directivity microstrip directional coupler, Schottky diode detector, two high gain RF buffers with controlled linearity - were specifically designed and optimized by the authors for manufacturing the temperature measurement system.*

**Keywords:** surface acoustic wave (SAW) resonator, temperature sensor

### 1. Introduction

Temperature sensors are widely used in many applications providing accurate temperature information that can be essential for proper environment condition or devices' functionality. Regular temperature measurement techniques utilize thermoelectricity, temperature dependent variation of the resistance of electrical conductors, fluorescence and spectral characteristics [1]. Temperature measurements are performed in direct contact with the medium (invasive), but non-contacting measurements are either possible for hostile environment or if certain device characteristics are affected [2]. In Table 1 are summarized the most used temperature measurements techniques and devices.

<sup>1</sup> Eng., National Institute for Research and Development in Microtechnologies, IMT- Bucharest, and University POLITEHNICA of Bucharest, Romania, e-mail: ioana.giangu@imt.ro

<sup>2</sup> PhD Eng., National Institute for Research and Development in Microtechnologies, IMT- Bucharest, Romania, e-mail: valentin.buiculescu@imt.ro

<sup>3</sup> Eng., National Institute for Research and Development in Microtechnologies, IMT- Bucharest, Romania, e-mail: mihai.nisulescu@imt.ro

<sup>4</sup> Prof., University POLITEHNICA - Bucharest, Romania, e-mail: george.lojewski@munde.pub.ro

Table 1

Main temperature measurement techniques and their performances [1]

No.	Measurement method	Temperature range [°C]		Sensitivity	Accuracy [°C]
		Minimum	Maximum		
1.	Liquid in glass thermometer	-200	600	1°C	±0.02 - ±10
2.	Thermocouple	-270	2300	10 $\mu$ V/°C	±0.5 - ±2
3.	Electrical resistance*	-260	1064	0.01 $\Omega$ /°C	±0.01
4.	Thermistor	-100	700	10 mV/°C	±0.01 - ±0.05
5.	Semiconductor devices**	-272	300	±1%	±0.1

\* Platinum (Pt) resistance thermometers

\*\* Silicon based sensors provide superior performance compared with so-called RTD (resistance-temperature-detectors), thermocouples and thermistors [3]

This paper is intended to give an overview of a novel and accurate scalar network analyzer (SNA) system type used for characterization of SAW (surface acoustic wave) resonators' behaviour as temperature sensors. This method, as proposed by the authors, is an inexpensive preliminary approach based on temperature information exclusively extracted from the reflected signal (parameter  $S_{11}$ ) of a SAW resonator, used before using the SAW device as ID tag in RFID-type wireless applications. The temperature information based on amplitude of a RF signal measurement corresponds to the return loss (RL) of a SAW resonator used as sensing element, while it is connected as terminal impedance of a transmission line with well defined characteristic impedance.

## 2. SAW temperature sensors

Radio Frequency Identification (RFID) technology has grown rapidly in the past few years as the need for automatic identification and tracking of goods has become increasingly important. SAW devices are successfully used in identification applications as ID tags, but also for measuring physical quantities such as temperature, pressure, humidity [4]. Because power supplies are not required in case of any SAW application, unlimited life time of these tags is expected. Furthermore, the SAW devices are compact, small, inexpensive, and easily fabricated [5], while they can work under harsh environment conditions.

Since the sensitivity of the humidity, mass or gas sensors is proportional to the square of the resonant frequency, or it is directly proportional to the resonant frequency for temperature and pressure sensors, a higher operating frequency of the acoustic wave sensors is obviously required [6]. Piezoelectric materials such as quartz, lithium niobate, lithium tantalite, langasite and langataate are normally used for manufacturing SAW resonators [6], but the propagation losses of these materials increase with frequency, thus limiting their operation up to about 2 GHz [7]. Only a few piezoelectric materials, for instance thin GaN layers grown on Si substrates, make possible the manufacturing of high performance SAW resonators working in the upper GHz range, even exceeding 5 GHz [6], [8]. Passive one-port

SAW resonators have also been widely studied and demonstrated high performances in terms of sensitivity and losses with increased quality factor  $Q$  [9].

The relative temperature sensitivity of a SAW resonator is defined using the resonance frequency  $f$  and absolute temperature of the device  $T$  [10] or, as a function of certain specific material and design parameters, i.e. sound velocity  $v$  inside the piezoelectric layer and distance  $L$  between adjacent fingers of the interdigital transducer (IDT):

$$S = \frac{1}{v} \frac{dv}{dT} - \frac{1}{L} \frac{dL}{dT} \quad (1)$$

The first term describing the propagation and the second term describing dilatation of (1) involve only the SAW resonator regions containing the IDT structure and reflectors. Because  $v \sim f$  and  $1/L \sim f$ , (1.b) points out an obvious advantage of the larger frequency shift as resonance frequency increases, for the same temperature change. A linear dependence of the surface acoustic wave velocity vs temperature results along thin layers of piezoelectric materials within regular temperature ranges, used in RFID-type wireless applications for temperature measurements [4] - [11].

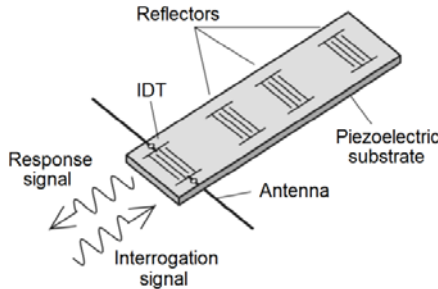


Fig. 1 General operating principle of SAW based sensing applications.

The most convenient way to obtain the temperature information from a SAW sensor consists in a wireless reading system using multiple reflection-based devices, as shown in Fig. 1 [12]. The incident RF signal's energy is transferred, by means of an interdigital transducer (IDT) located over a piezoelectric layer, to an acoustic wave which starts to propagate along the piezoelectric structure. During propagation, the acoustic wave is reflected partly by each reflector element located at a certain distance from IDT, due to a controlled transparency coefficient to the acoustic wave. Therefore, the resultant wave occurring at the antenna port contains the vectorial sum of all reflected waves which is backscattered into surrounding space. However, SAW resonators with resonance frequencies exceeding a few GHz have extremely high transmission losses, therefore signal amplitudes after multiple reflections from inner reflectors become too small to remain suitable for accurate information extraction. As a single, non-reflective

SAW resonator is intended for temperature measurements, an analysis of this device in a „wired” connection allows the observation of some of its specific response properties.

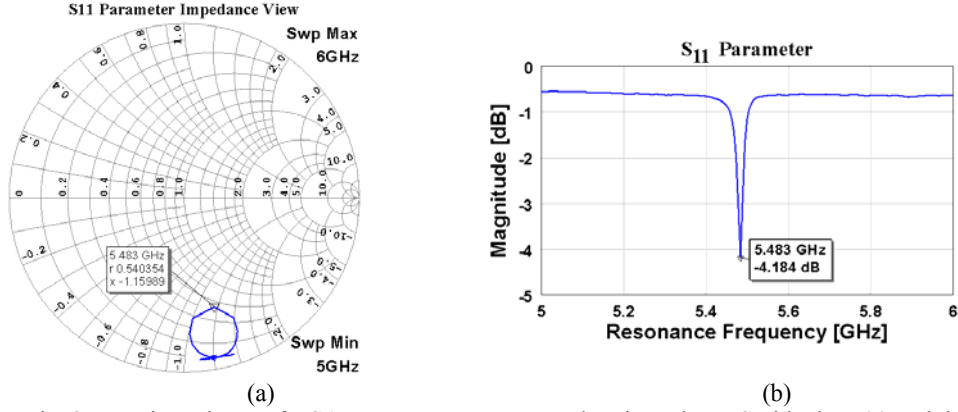


Fig. 2 Input impedance of a SAW resonator represented on impedance Smith chart (a) and the corresponding return loss modulus expressed in dB (b).

Plotted on impedance Smith chart, the input impedance of a SAW resonator has a specific loop-like pattern shown in Fig. 2.a, practically observed on all SAW resonators [13], [14]. In terms of return loss (RL), the same impedance evolution changes its representation (Fig. 2.b) into an almost constant value over a broad bandwidth, interrupted by a V-shaped section with a minimum value corresponding to the point closest to the centre of the circle observed in case of the previous diagram. The frequency corresponding to the minimum RL is extremely close to the shunt resonance of the SAW [14], therefore it follows accurately the temperature behavior of the original resonator. This specific response has suggested a new measurement procedure for ambient temperature, using the return loss scalar representation of a SAW sensor connected as load impedance for a transmission line of  $50 \Omega$  characteristic impedance.

### 3. System description and development

The corresponding block diagram of the proposed measurement system (Fig. 3) consists of two main signal paths - each filled with a specific color - interconnected by a high directivity directional coupler loaded with the SAW temperature sensor at a specific port.

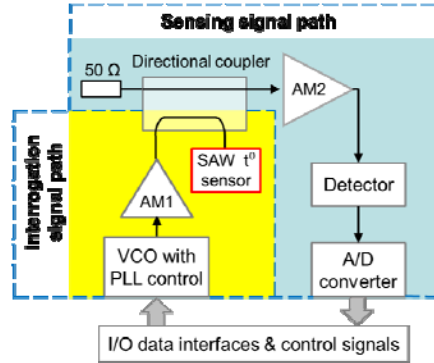


Fig. 3 Simplified block diagram of the measurement system.

The *interrogation path* provides a RF signal swept in programmable steps that cover a frequency band exceeding the expected resonance frequency shift of the SAW sensor over specified temperature range of the system. The RF signal is generated by a voltage controlled oscillator (VCO) within a phase-controlled loop (PLL) for accurate frequency settling and stabilization. A group of broadband amplifiers (AM1) provides both good isolation of the VCO's output port from an almost purely reactive SAW sensor's input impedance and improved amplitude stability of the interrogation signal. The temperature sensor is a single-port SAW resonator with 5.3 - 5.65 GHz resonance frequency at room temperature, and about 350 kHz/°C sensitivity [15].

A directional coupler is used to send the signal containing the temperature information, as it is reflected by the SAW resonator, towards the second major RF path (*signal sensing path*) for further processing. The input amplifier chain of this path (AM2) increases the RF signal level until it reaches a large value at the input of a Schottky diode peak detector. The variable voltage at the detector output, containing information about temperature dependent reflection coefficient of the SAW sensor, enters the analog-to-digital (A/D) converter for providing the measured data in a specific format for storage into a computer memory.

### 3.1. Directional coupler

Directional coupler's characteristics essential for our specific application are the directivity  $D$  and coupling factor  $C$ . Of these,  $D$  has to be as high as possible, since it contributes to the isolation between the signal reflected from the SAW temperature sensor and fraction of the interrogation signal incident to the signal sensing path, as required by a uniform system response over large bandwidths. On the other hand, a tight coupling factor  $C$  is beneficial for lowering the complexity of the system, whose internal structure and signal power levels in the key points are directly related to it. However, some technical constraints

establish a lower limit for  $C$ , therefore its minimum available value has to be determined before designing the rest of the system.

Table 2

Main directional coupler characteristics used during optimization.

No.	Parameter	Value
<i>a) Material parameters</i>		
1.	Substrate height ( $h$ )	1.6 mm
2.	Substrate permittivity ( $\epsilon_r$ ) - typical value	4.3
3.	Copper thickness ( $t$ )	0.035 mm
<i>b) Layout specific value</i>		
4.	Minimum gap width	0.625 mm
<i>c) Electrical parameters</i>		
5.	Coupling factor ( $C$ ) - mean value	13.5 dB
6.	Minimum bandwidth ( $BW$ )	4.7 - 6.2 GHz

The main limitation during our design occurred due to the gap width  $s$  between transmission lines in the coupling zone. The minimum value of about  $s = 0.35$  mm was further correlated with relative permittivity  $\epsilon_r$  and thickness  $h$  of the substrate, thus defining the minimum available  $C$  [16]. Although increasing both these values provide a lower  $C$ , the signal line widths become too large to remain compatible with SMA connectors used for all RF sub-systems, therefore a regular 1.6 mm thick FR-4 substrate was considered for manufacturing. In order to obtain a large bandwidth, a three-section structure was designed and optimized, with relevant parameters presented in Table 2. It is noticed a gap width  $s = 0.625$  mm, larger than minimum specification of 0.35 mm, because the relative manufacturing accuracy is better for this limit, obviously helpful for coupler's directivity.

### 3.2. Interrogation signal path

The interrogation path contains all circuits required to provide a RF signal with stable amplitude and frequency over full operating band of the system. The most important components of this sub-system are (i) a broadband tunable voltage controlled oscillator (VCO) and (ii) a high performance programmable frequency synthesizer used for optimum VCO control. A second-order low-pass filter closes the resulting phase locked loop (PLL) in a specific connection (Fig. 4). By means of a USB connection, the programmable synthesis circuit allows for an optimized frequency sweep with variable steps according to the required reading resolution.

The multiple-output VCO used in our application has 10.5 - 12.1 GHz nominal output frequency, with additional output signals obtained after frequency division by two and four. The signal covering 5.25 - 6.05 GHz band is used for sensor's interrogation, since this band is common with the resonance frequency of the SAW sensors, while the lower frequency signal controls the synthesizer,

which has a maximum operation frequency of about 4 GHz. Adaptive frequency steps - within 10 kHz up to 1 MHz range - are available for accurate searching of the minimum amplitude response corresponding to the measured temperature.

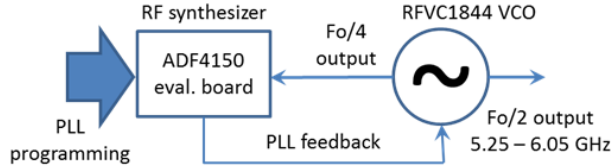


Fig. 4 PLL controlled VCO - block diagram

Both frequency and nominal output power of the VCO is normally maintained stable if the load impedance of this circuit is predominantly resistive, otherwise the load pulling can occur. The actual impedance of the SAW resonator, with a high quality factor  $Q$ , is normally improper to load directly the VCO. Due to this reason, additional circuits and components were inserted in our design between VCO and the SAW device for reducing the influence of the specific resonator's impedance upon system's stability. The solution chosen for this purpose uses a RF chain based on amplifier stages with uniform broadband gain and a few attenuator pads. Therefore, constant amplitude of the interrogation signal over full operation bandwidth and high signal level for compensating the signal losses due to finite coupling factor  $C$  are obtained.

Table 3

Typical parameters of the integrated amplifier SBB-3089Z [17]

No.	Parameter	Unit	SBB-3089Z
1.	Power gain	dB	16
2.	Working bandwidth	GHz	0.1...6
3.	Output power at 1 dB compression	dBm	+15
4.	Input return loss (maxim)	dB	-10
5.	Output return loss (maxim)	dB	-17
6.	Device operating voltage	V	4.2
7.	Device operating current (typical value)	mA	42

A monolithic integrated amplifier SBB-3089Z model was chosen to answer the above signal level requirements along each signal path. The main characteristics of this device (Table 3) show a good intrinsic impedance matching at both signal ports and excellent reverse isolation. The amplifier requires simple bias and decoupling circuits, so an inductor and two RF coupling capacitors with values optimized for the actual frequency bandwidth have been used. Since the output power available from the VCO is about +9 dBm, while the output power for 1 dB compression of SBB-3089Z is typically 15 dBm, the current block diagram of AM1 has the structure presented in Fig. 5.

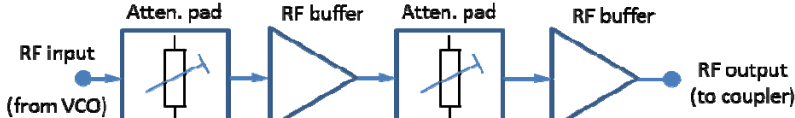


Fig. 5 AM1 structure

Two amplifier stages are used for (i) increasing the interrogation signal's level close to 1 dB compression limit and (ii) for compensating the signal losses due to gain adjusting attenuators. The attenuators are inserted between stages in order to improve the impedance matching at both signal ports of the complete amplifiers, because single stages are not perfectly matched. In addition, the total gain of the signal path is "tuned" in order to obtain a weak signal compression, therefore maintaining almost constant the level of the signal used for the SAW resonator interrogation. This controls to a certain extent the generation of harmonic content of the fundamental frequency signal due to nonlinearities of the active components at high input signal levels.

### 3.3. Sensing signal path

The signal reflected by the SAW resonator used as temperature sensor is picked-up from the coupled port of the directional coupler for further processing in the second RF block in the sensing signal path. Taking into account the coupling factor  $C$  and the amplitude of the reflected by the SAW resonator, the typical power levels at the input of AM2 are within  $-7 \dots -15$  dBm range. Since any signal distortion or compression can affect the dynamic range of the whole sensing path, thus affecting the system's accuracy, all amplifier stages have to work as linearly as possible.

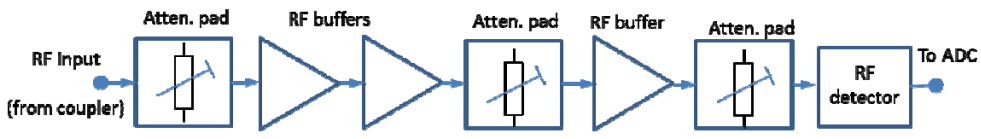


Fig. 6 Current structure of AM2

Although the electrical parameters are quite similar for both AM1 and AM2, the last item has a different configuration, with an extra amplifier stage and, correspondingly, higher value attenuators distributed along AM2 chain (Fig. 6). This solution improves overall  $S_{12}$  value, because impedance matching is more stringently required as  $S_{11}$  of this chain represents the actual load impedance of the SAW resonator. For this reason, a structure similar to the AM1 has to be used for AM2, i.e. with amplifiers and attenuators for fine trimming the gain and power levels inside the path. Therefore, a three-stage amplifier chain with inter-stage

attenuators avoids the stability issues due to impedance mismatch of the RF detector. This is required due to relaxed specifications for detector's matching, while providing a good signal/noise ratio to the Schottky diode detector, before analog-to-digital (A/D) conversion. An operational amplifier may be placed between detector's output and the A/D converter, in order to increase the DC voltage level for a higher resolution A/D converter.

#### 4. Experimental results

Certain electrical characteristics of the main blocks used in the temperature measuring system are closely interrelated, therefore each functional block was carefully evaluated as independent part, before it was connected in the final structure. Therefore, both impedance matching and fine tuning of the gain in order to fulfill specific linearity requirements described above were verified and adjusted for each amplifier block, in order to address the linearity requirements of each amplifier chain. Due to the weak compression used in AM1, the amplitude response of full interrogation path, from VCO's output port to the SAW sensor, has an excellent flatness of 0.2 dB over 200 MHz bandwidth; the second harmonic content due to compression does not exceed  $-20$  dBc. As stated above, the linearity of AM2 has to be very good, for maintaining the maximum available dynamic range of this amplifier.

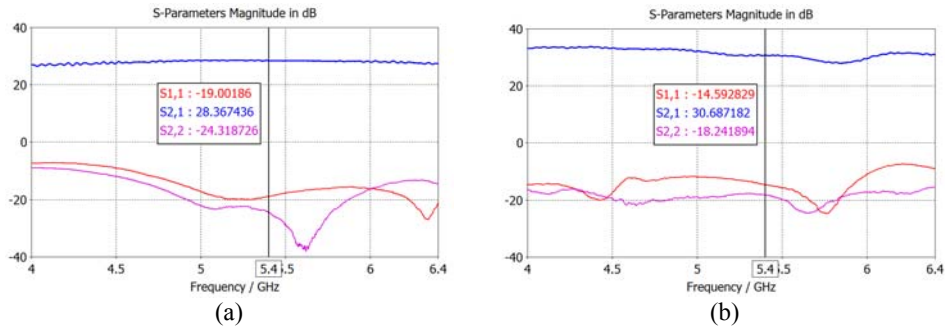


Fig. 7 Experimental results for: (a) two stage amplifier and (b) three stage amplifier

The experimental results obtained for two and, respectively, three stage amplifiers are shown in Fig. 7. Because the gain is high for both circuits, all determinations were performed at an input signal power of  $-25$  dBm, in order to avoid the entering into limitation of these circuits during their evaluation. Reverse transmission coefficient ( $S_{12}$ ) of the amplifier AM1 is better than  $-43$  dB and also better than  $-55$  dB for AM2 in actual configurations, thus confirming the assumption made about amplifier model choice and structural solution. One can see also a very good impedance matching at both ports, with good uniformity of the gain over large bandwidths of each amplifier version.

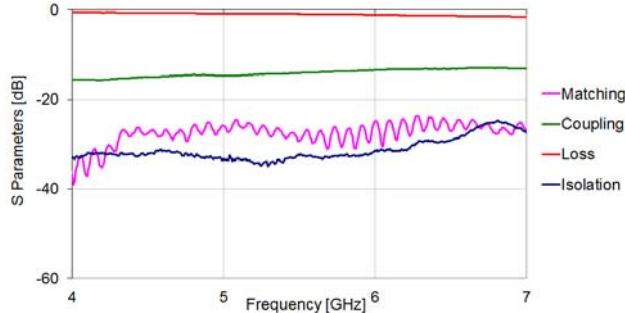


Fig. 8 Broadband characteristics of the directional coupler

The input port of the directional coupler receives a RF signal from the interrogation path. The experimental results presented in Fig. 8 show a very good impedance matching (magenta curve) and a coupling factor of about  $-14 + 0.5$  dB over a broad bandwidth centered around 5 GHz wireless communication band (green curve), used for this application. Also, the coupler's directivity of about 20 dB results from manufacturing accuracy and consequent excellent impedance matching over the same broad bandwidth.

The RF detector that follows after AM2 block consists of a Schottky diode and a RF decoupling capacitor placed at the detector's output. A single  $100\ \Omega$  input resistor is used instead of reactive matching networks, mainly due to the excellent reverse isolation of AM2. The detector's DC response depends on the input RF power applied from a microwave signal generator. The quadratic response i.e. the output DC voltage is proportional to the input microwave power signal, was observed for a signal lower than about  $-10$  dBm, and linear response, with output DC voltage proportional to the voltage amplitude of the RF signal, was measured for a power level higher than 0 dBm.

Temperature characterization of the SAW resonator was performed in a controlled temperature enclosure (oven) allowing a settling accuracy better than  $1^\circ\text{C}$ . Forced air circulation ensures uniform temperature distribution inside the oven, regardless measured device's positioning. The connection between the SAW sensor, located inside the oven, and the directional coupler placed along with other components of the SNA (outside the oven) is carried out through a coaxial cable. After A/D conversion, the corresponding data is recorded in binary form in the computer's memory. The measurement results for several temperatures are shown in Fig. 9. One can see small fluctuations of the voltage measured at the detector's output. These variations can be explained as a consequence of the finite resolution of the A/D converter, with some contributions from low frequency electrical noise picked-up due to improper shielding within DC processing path (wire connections between detector and converter).

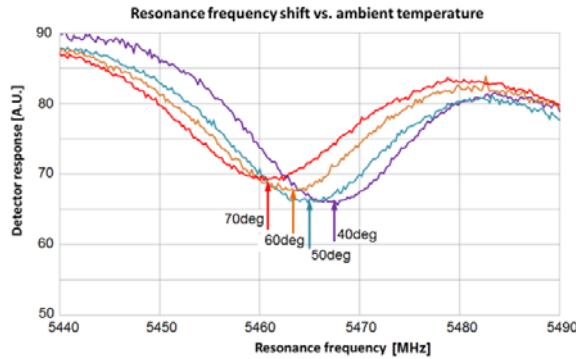


Fig. 9 Temperature response of the SAW temperature sensor measured with complete system

## 5. Conclusions

A very simple temperature measuring system has been developed using a few readily available RF components and custom designed circuits like the directional coupler, two and three stage RF amplifiers, Schottky diode detector and the A/D converter. For temperature sensing, a GaN/Si based SAW structure operating at 5.4 GHz has been used due to its high sensitivity (about 350 kHz/°C). A directional coupler with a very good impedance matching, coupling factor of about  $-14 \pm 0.5$  dB and a directivity of about 20 dB was designed. The RF buffers have shown a very good impedance matching at both ports, with good uniformity of the gain. A VCO tunable over a large frequency bandwidth covering 5.25 - 6.05 GHz band was used for sensor's interrogation and a programmable frequency synthesizer have been used for generating the signal required to cover the corresponding SAW resonator operating frequency band. Laboratory-grade equipment - vector network analyzer, signal generator and spectrum analyzer - was used for RF characterization of the circuits. RF-to-DC conversion characteristics of the detector were measured with an RF generator and broadband oscilloscope. After the complete system was assembled, the processed data gave the typical response of the SAW temperature sensor. Further signal processing refinement and adaptive frequency sweep can improve the reading accuracy.

## Acknowledgment

The authors acknowledge the support of the EC under Integrated FP7 Project SMARTPOWER, FP7 grant agreement 288801/2011-2014. The author Ioana Giangu acknowledges also the support of the Sectoral Operational Programme Human Resources Development 2007-2013 of the Ministry of European Funds through the Financial Agreement POSDRU/159/1.5/S/132397.

## R E F E R E N C E S

- [1]. *P.R.N. Childs, J.R. Greenwood, and C.A. Long*, „Review of temperature measurement (Review article)”, Review of Scientific Instruments, **vol. 71**, no. 8, 2000, pp. 2959-2978
- [2]. *M. A. Khan, C. Allemand and T. W. Eagar*, “Non contact temperature measurement. I. Interpolation based techniques”, Rev. Sci. Instrum., **vol. 62**, no. 2, 1991, pp. 392-402
- [3]. *D. J. Kunst*, “Solid State Temperature Measurement”, United States Patent, Kunts, 1999
- [4]. *V. P. Plessky, L. M. Reindl*, “Review on SAW RFID Tags”, IEEE Transactions on Ultrasonics, Ferroelectrics and Frequency Control, **vol. 57**, no. 3, 2010, pp. 654 – 668
- [5]. *U. Wolff, F. L. Dickert, G. K. Fischerauer, W. Greibl, and C.C.W. Ruppel*, “SAW Sensors for Harsh Environments”, IEEE Sensors Journal, **vol. 1**, no. 1, 2001, pp. 4-13
- [6]. *A. Müller, G. Konstantinidis, V. Buiculescu, A. Dinescu, A. Stavriniidis, A. Stefanescu, G. Stavriniidis, I. Giangu, A. Cismaru, A. Modoveanu*, “GaN/Si based single SAW resonator temperature sensor operating in the GHz frequency range”, Sensors and Actuators A: Physical, **vol. 209**, 2014, pp. 115-123
- [7]. *A. Müller, G. Konstantinidis, I. Giangu, V. Buiculescu, A. Dinescu, A. Stefanescu, A. Stavriniidis, G. Stavriniidis, A Ziae*, “GaN-based SAW structures resonating within the 5.4-8.5 GHz frequency range, for high sensitivity temperature sensors” International Microwave Symposium-IMS, Tampa, USA, session “TH2F: Sensors and Sensor Systems”, 2014, pp 46-48
- [8]. *A. Müller, D. Neculoiu, G. Konstantinidis, G. Deligeorgis, A. Dinescu, A. Stavriniidis, A. Cismaru, M. Dragoman, A. Stefanescu*, “SAW devices manufactured on GaN/Si for frequencies beyond 5 GHz”, Electron Devices Letters, **vol 31**, no. 12, 2010, pp. 1398-1400
- [9]. *X. Ye, Q. Wang, Lu Fang, X. Wang, Bo Liang*, “Comparative Study of SAW Temperature Sensor Based on Different Piezoelectric Materials and Crystal Cuts for Passive Wireless Measurement”, IEEE Sensors Conference, 2010, pp. 585-588
- [10]. *F. Calle, J. Pedrós, T. Palacios, J. Graja*, “Nitride-based surface acoustic wave devices and applications”, Phys. Stat. Sol., **vol.2**, 2005, pp. 976–983
- [11]. *A. Kang, C. Zhang, X. Ji, T. Han, R. Li, and X. Li*, “SAW-RFID enabled temperature sensor,” Sensors and Actuators A, **vol. 201**, 2013, pp. 105– 113
- [12]. *S. Schuster, S. Scheiblhofer, L. Reindl, A. Stelzer*, “ Performance evaluation of algorithms for SAW-based temperature measurement”, IEEE Trans. Ultrason., Ferroelectr., Freq. Control, **vol. 53**, no. 6, 2006, pp. 1177-1185
- [13]. *David Morgan*, “Surface Acoustic Wave Filters”, Elsevier Ltd., Second Edition, 2007
- [14]. *K. M. Lakin, G. R. Kline, K. T. McCarron*, “High-Q Microwave Acoustic Resonators and Filters”, IEEE Trans. Microw. Theory Tech., **vol. 41**, no.12, 1993, pp. 2139-2146
- [15]. *I. Giangu, V. Buiculescu, G. Konstantinidis, K. Szaciłowski, A. Ștefănescu, F. Bechtold, K. Pilarczykd, A. Stavriniidis, P. Kwolek, G. Stavriniidis, J. Mech and A. Müller*, “Acoustic wave sensing devices and their LTCC packaging”, Annual Semiconductor Conf., CAS 2014, Sinaia, Romania, October 2014, pp. 147-150
- [16]. *G.L. Matthaei, L. Young, and E.M.T.Jones*, “Microwave filters, impedance-matching networks, and coupling structures”, McGraw-Hill (Publ.), 1964, section 13.03
- [17] [http://www.rfmd.com/store/downloads/dl/file/id/28146/sbb3089z\\_data\\_sheet.pdf](http://www.rfmd.com/store/downloads/dl/file/id/28146/sbb3089z_data_sheet.pdf)